Acta Crystallographica Section D
Biological Crystallography
ISSN 0907-4449

Mutational and structural studies of the active-site residues in truncated *Fibrobacter succinogenes* 1,3–1,4-β-D-glucanase

Li-Chu Tsai,[a]* Hsiao-Chuan Huang,[a] Ching-Hua Hsiao,[a] Yuan-Neng Chiang,[a] Lie-Fen Shyur,[b]* Yu-Shiun Lin[b] and Shu-Hua Lee[b]

[a]Department of Molecular Science and Engineering, National Taipei University of Technology, Taipei 106, Taiwan, and [b]Agricultural Biotechnology Research Center, Academia Sinica, Taipei 115, Taiwan

Correspondence e-mail: lichu@ntut.edu.tw, lfshyur@ccvax.sinica.edu.tw

Received 31 July 2008
Accepted 14 October 2008

PDB Reference: 1,3–1,4-β-D-glucanase, E85I mutant, 2r49, r2r49sf.

1,3–1,4-β-D-Glucanases (EC 3.2.1.73) specifically hydrolyze β-1,4-glycosidic bonds located prior to β-1,3-glycosidic linkages in lichenan or β-D-glucans. It has been suggested that truncated *Fibrobacter succinogenes* 1,3–1,4-β-D-glucanase (TFsβ-glucanase) can accommodate five glucose rings in its active site upon enzyme–substrate interaction. In this study, 12 mutant enzymes were created by mutating the conserved residues Gln70, Asn72, Gln81 and Glu85 proposed to bind to substrate subsites +1 and +2 and the catalytic properties of these mutants were determined. The most significant change in catalytic activity was observed on mutation of Gln70, with a 299-fold and 498-fold lower k_{cat}/K_m for the mutants Q70A and Q70I, respectively, compared with the wild-type enzyme. Mutagenesis, kinetic and structural studies revealed that the conserved residues surrounding the active site of TFsβ-glucanase at substrate subsites +1 and +2 play an important role in its catalytic function, with the following order of importance: Gln70 > Asn72 > Glu85 > Gln81. The crystal structure of mutant E85I was determined at 2.2 Å resolution. Further analysis of the E85I mutant structure revealed that the loop located at the concave site moved approximately 2 Å from its position in the native enzyme complex without changing the core structure.

1. Introduction

The recognition of carbohydrates by proteins in important biological processes such as the degradation, modification or creation of glycosidic bonds involves a range of molecular interactions. In particular, the noncovalent interactions hydrogen bonding and van der Waals forces play a major role in protein–protein and protein–substrate stabilization (Cerny & Hobza, 2007; Li *et al.*, 2008; Sacquin-Mora *et al.*, 2008). The important industrial enzyme family glycosyl hydrolases recognize and bind particular carbohydrates and then cleave a specific glycosidic bond between two or more carbohydrates utilizing two major hydrolytic mechanisms: inversion and retention. Three general active-site topologies of glycosyl hydrolases are known, namely pocket, cleft and tunnel, for the recognition of various carbohydrates (Davies & Henrissat, 1995). The glycosidic bond is hydrolyzed by two catalytic residues of the enzyme: a general acid/base and a nucleophile/base (Davies & Henrissat, 1995). In most cases, glycoside hydrolases do not require any cofactor/coenzyme to hydrolyze the spatial glycosidic bond; they generally use two catalytic residues, glutamate or aspartate, of the enzyme. In some cases, the catalytic nucleophile is not borne by the enzyme and is replaced by the acetamido group at C-2 of the substrate (Rao *et al.*, 2006; Dennis *et al.*, 2006). However, a novel unrelated

Table 1
Oligonucleotide primers for site-directed mutagenesis.

Mutant	Sequences of mutagenic primer
Q70A	5′-GCAGTTTC**GCG**TCCAACATC-3′
Q70D	5′-GGCAGTTTC**GAC**TCCAACATC-3′
Q70E	5′-GCAGTTTC**GAG**TCCAACATC-3′
Q70I	5′-CCGGGCAGTTTC**ATC**TCCAACATCA-3′
Q70N	5′-CGGGCAGTTTC**AAC**TCCAACATCA-3′
Q70R	5′-GGCAGTTTC**CGG**TCCAACATC-3′
N72A	5′-GTTTCCAGTCC**GCC**ATCATTACCG-3′
N72Q	5′-GTTTCCAGTCC**CAG**ATCATTACCGG-3′
Q81I	5′-GGCCGGCGCA**ATA**AAGACTAGC-3′
Q81N	5′-GGCCGGCGCA**AAC**AAGACTAGCG-3′
E85D	5′-AAGACTAGC**GAC**AAGCACCATG-3′
E85I	5′-CAAAAGACTAGC**ATA**AAGCACCATGC-3′

mechanism reported for family 4 glycosidases involves NAD^+/Mn^{2+} as a cofactor (Rajan *et al.*, 2004).

1,3–1,4-β-D-Glucanases (EC 3.2.1.73) specifically hydrolyze and cleave β-1,4-glycosidic bonds at β-1,4-glycosidic linkages before β-1,3-glycosidic linkages in lichenan or β-D-glucans (Anderson & Stone, 1975) *via* a retention cleavage mechanism (Davies & Henrissat, 1995). β-D-Glucans are a major cell-wall component of endosperm tissues in cereal grains. Supplementation of animal feed with 1,3–1,4-β-D-glucanase is one approach that has been used to increase the feed-conversion efficiency and growth rate of non-ruminant animals such as poultry (Bedford *et al.*, 1992; Selinger *et al.*, 1996). The feasibility of using this enzyme in agriculture and other bio-industrial applications has promoted studies of its structure–function relationship. 1,3–1,4-β-D-Glucanases are present in various bacteria, fungi and plant tissues (Henrissat, 1991; Henrissat & Bairoch, 1993; Keitel *et al.*, 1993; Chen *et al.*, 1997). The crystal structures of 1,3–1,4-β-D-glucanases from *Bacillus licheniformis* (Bs; Hahn *et al.*, 1995), *Fibrobacter succinogenes* (Fs; Tsai *et al.*, 2003) and *Paenibacillus macerans* (Pm; Keitel *et al.*, 1993) exhibit a jelly-roll β-sandwich fold with a cleft active site and have been classified into glycosyl hydrolase family 16 (GHF16). Barley 1,3–1,4-β-D-glucanase, which folds into a $(\beta/\alpha)_8$ motif (Varghese *et al.*, 1994; Müller *et al.*, 1998) with a pocket active site, is a member of GHF17 (http://www.cazy.org/fam/acc_GH.html). The 1,3–1,4-β-D-glucanases from Pm (Gaiser *et al.*, 2006) and Fs (Tsai *et al.*, 2005) have been most studied in terms of the enzyme–product crystal structure. Although the sequences of Fsβ-glucanases only have ~30% amino-acid sequence identity to Bs and Pmβ-glucanases, the enzymes show a high degree of structural conservation in the active site, with 13 of the 18 binding residues being similar (Tsai *et al.*, 2005). This may imply that these enzymes share a similar active-site topology for substrate recognition and binding. The structure of the complex of a β-1,4–1,3-cellotriose (CLTR) in the active cleft of truncated Fsβ-glucanase (TFsβ-glucanase) has been determined (Tsai *et al.*, 2005) and modelling of an extension comprising the additional carbohydrate subunits +1 and +2 in this complex (Tsai *et al.*, 2008) suggested that residues Asp58, Gln70, Asn72, Gln81, Glu85 and Trp148 of TFsβ-glucanase are associated with subunits +1 and +2 of the bound carbohydrate substrate.

To gain further insight into protein–substrate interactions and catalytic mechanisms in 1,3–1,4-β-D-glucanase, in this study we mutated the relevant residues Gln70, Asn72, Gln81 and Glu85 and characterized the catalytic activity of the mutants by determining the rate of reducing-oligosaccharide production from hydrolysis of the substrate lichenan. Mutation of these specific residues significantly attenuated the catalytic efficiency of TFsβ-glucanase by 20–99%. To study whether replacement with a specific amino acid has a possible structural effect on the protein that consequently affects the enzymatic activity, we further investigated the crystal structure of the E85I mutant determined at 2.2 Å resolution. X-ray diffraction data showed that in the E85I mutant the four loops shifted away from the concave site, which caused the residue Trp148 located in one of the shifted loops to move away from the active site, thus forcing Glu60 and Gln70 to also move approximately 2.2 Å away from the active site. From these biochemical and structural results, we suggest that the conserved residues Asp58, Gln70, Asn72, Gln81, Glu85 and Trp148 located around subunits +1 and +2 of the bound carbohydrate play important structural roles in maintaining the conformation of the substrate-binding site and in interaction with the substrate.

2. Materials and methods

2.1. Site-directed mutagenesis, expression and purification of enzyme mutants

A plasmid carrying the truncated *F. succinogenes* 1,3–1,4-β-D-glucanase gene in the pET26b(+) vector was amplified by PCR (Chen *et al.*, 2001). In this study, we created a series of mutant forms of TFsβ-glucanase, including Q70A, Q70D, Q70E, Q70I, Q70N, Q70R, N72A, N72Q, Q81I, Q81N, E85D and E85I mutants, using specifically designed mutagenic primers (Table 1). The PCR products were incubated with 10 units of *Dpn*I at 310 K for 1 h to digest the DNA template and were then transformed into *Escherichia coli* XL1-Blue. For the overexpression of mutant enzymes, plasmids bearing the desired mutation were transformed into *E. coli* BL21 (DE3) cells, cultured in LB medium (30 µg ml^{-1} kanamycin) to an OD_{600} of 0.6 and then induced with 1 m*M* isopropyl β-D-1-thiogalactopyranoside at 307 K for 16 h. The supernatant was harvested and 1 m*M* phenylmethanesulfonyl fluoride and 1 µg ml^{-1} leupeptin were added to avoid enzymatic degradation. Subsequently, the medium was concentrated to one-tenth of the original volume using a Pellicon Cassette concentrator with a 10 000 Da molecular-weight cutoff membrane. 10 m*M* imidazole and 0.3 *M* NaCl were added to the concentrated protein solution and it was applied onto an Ni–NTA affinity column (Pharmacia). After washing with 50 m*M* sodium phosphate buffer pH 8.0 containing 20 m*M* imidazole and 0.3 *M* NaCl, the mutant protein was eluted with a linear gradient of 20–250 m*M* imidazole in the same buffer. The purified mutant proteins were analyzed by Coomassie-stained SDS–PAGE and zymography to monitor protein purity and mutant activity (Wen *et al.*, 2005). Protein fractions of more

Table 2
Data-collection and refinement statistics of the E85I mutant.

Values in parentheses are for the last shell.

Data collection and processing	
Space group	$P3_121$
Unit-cell parameters (Å, °)	$a = b = 69.6$, $c = 97.4$, $\alpha = \beta = 90.0$, $\gamma = 120.0$
Resolution (Å)	2.2 (2.28–2.2)
Observed reflections	79053
Unique reflections	14319
Completeness (%)	99.6 (98.9)
$R_{\rm merge}$†	9.8 (24.2)
$I/\sigma(I)$	14.2 (8.1)
Refinement	
Resolution range (Å)	50.0–2.2
Reflections	14182
Non-H atoms	
Protein	1900
Calcium ion	1
Caesium ion	1
Solvent molecules	199
R factor‡ (%)	19.6
$R_{\rm free}$ (%)	26.6
Model quality	
R.m.s. deviations	
Bond lengths (Å)	0.013
Bond angles (°)	1.78
Average B factors (Å^2)	
Protein atoms	28.1
Solvent atoms	35.3
Ramachandran plot (%)	
Most favoured	87.3
Additionally allowed	11.2
Generously allowed	0.5
Disallowed	1.0

† $R_{\rm merge} = \sum_{hkl}\sum_i |I_i(hkl) - \langle I(hkl)\rangle| / \sum_{hkl}\sum_i I_i(hkl)$. ‡ R factor $= \sum_{hkl} \big||F_{\rm o}(hkl)| - |F_{\rm c}(hkl)|\big| / \sum_{hkl} |F_{\rm o}(hkl)|$.

than 95% purity were dialyzed against 50 m*M* sodium phosphate buffer pH 7.0 at 277 K, concentrated and then stored with the addition of 10% glycerol at 253 K.

2.2. Kinetic analysis

The enzymatic activities of the purified TFsβ-glucanase and mutants were measured by determining the rate of reducing-sugar production from hydrolysis of the substrate lichenan (molecular weight 139 000 Da; Sigma). Reducing sugars were quantified by the use of 3,5-dinitrosalicylic acid reagent (Miller, 1959) with glucose as the standard. Enzyme-activity assays were carried out in 0.3 ml reaction mixtures containing lichenan at the optimal pH of each enzyme mutant. After incubation at an optimal temperature for 10 min, the enzyme reaction was terminated by the addition of 0.6 ml 3,5-dinitrosalicylic acid reagent (1% 3,5-dinitrosalicylic acid, 0.2% phenol, 1% NaOH; Miller, 1959) and incubated at 368 K for 10 min. Finally, 0.15 ml 40% sodium potassium tartrate solution was added to the reaction mixtures, which were then allowed to cool at ambient temperature for 15 min, after which the absorbance at 575 nm was recorded. One unit of enzyme activity was defined as the amount of enzyme required to release 1 µmol of reducing sugar (glucose equivalent). The specific activity was expressed in micromoles of glucose per minute per milligram of protein. Kinetic data were analyzed using *EnzFitter* (Biosoft).

2.3. Calcium-ion analysis

The concentration of calcium ions in the mutant proteins was measured by polarized Zeeman atomic absorption spectrophotometry (PZAAS; Hitachi/Z-6100). Firstly, 20 µl mutant protein (at 10 mg ml^{-1}) was mixed with 10 ml 65% nitric acid in a flask covered with a watch glass and heated to 368 K for 4 h. After the digestion, the flasks were left to cool, transferred to volumetric flasks and diluted to 10.0 ml with deionized water. Blank and standard-curve samples used exactly the same procedure as for the test samples. The analytical wavelength was set to 595 nm and concentrations were obtained directly from calibration graphs after correction of the absorbance for the signal from an appropriate reagent blank.

2.4. Crystallization and X-ray data collection

Crystallization of the TFsβ-glucanase mutant proteins took place using the hanging-drop vapour-diffusion method at room temperature. Prior to crystallization, the purified protein was concentrated to 10 mg ml^{-1} in 10 m*M* Tris–HCl buffer pH 7.5. Crystals of the E85I protein were grown in a reservoir buffer solution containing 30%(*w*/*v*) PEG 6000, 0.1 *M* CsCl and 0.1 *M* MES pH 5.6. Crystals appeared after one week and reached final dimensions of approximately 1 × 0.1 × 0.02 mm. Crystals were soaked in cryoprotectant (10% glycerol in reservoir solution) for 1 min before data collection. X-ray diffraction data sets (Table 2) were collected at low temperature (~123 K) using an R-AXIS-IV^{++} imaging plate equipped with a confocal-mirror focusing system mounted on a rotating-anode X-ray generator (Micro-Max007, MSC Co., Bethesda, Maryland, USA). Indexing and integration of diffraction data were performed using *DENZO* and *SCALEPACK* (Otwinowski & Minor, 1997). E85I crystals diffracted X-rays to a resolution of 2.2 Å. The diffraction statistics are listed in Table 2.

2.5. Structure determination and refinement

The E85I mutant structure was solved by molecular replacement, using the previously determined $P2_12_12_1$ structure of TFsβ-glucanase (PDB code 1mve) as the search model. Cross-rotation and translation functions generated by the program *CNS* clearly identified one unique peak in the asymmetric unit (Brünger *et al.*, 1998). Rigid-body refinement gave an R factor of 31.1%. Further anisotropic refinement with simulated annealing was carried out using the program *CNS* for all data to 2.2 Å resolution. 10% of the observed reflections were randomly selected and used to calculate $R_{\rm free}$ during the refinement process. At this stage, electron density at the mutation site was clearly seen. Manual rebuilding of the model and the addition of solvent molecules were performed using *TURBO* (Roussel & Cambillau, 1992). The final refined statistical parameters for E85I are listed in Table 2.

3. Results and discussion

3.1. Enzymatic function and hydrolytic activity

Seven residues, Asp58, Glu60, Gln70, Asn72, Gln81, Glu85 and Trp148, located at the active site of TFsβ-glucanase have been proposed to bind to substrate subsites +1 and +2 of carbohydrate β-D-glucans or lichenan (Fig. 1; Tsai *et al.*, 2008). Of these residues, the kinetic functions of Asp58, Glu60 and Trp148 have been studied previously (Chen *et al.*, 2001; Cheng *et al.*, 2002). The activities of the D58A and E60A mutants were not detectable, whereas the W148F mutant showed a sixfold decrease in catalytic efficiency. In this study, we created a series of mutant forms of TFsβ-glucanase, including Q70A, Q70D, Q70E, Q70I, Q70N, Q70R, N72A, N72Q, Q81I, Q81N, E85D and E85I, using specifically designed mutagenic primers. Wild-type and 12 mutant TFsβ-glucanases were effectively expressed in *E. coli* BL21 (DE3) host cells upon induction with 1 m*M* IPTG at 306 K. The TFsβ-glucanases all contained a *pel* leader sequence at the N-terminus and a His tag at the C-terminus and were expressed extracellularly into culture medium and purified using an Ni–NTA affinity column. The homogeneity of each purified mutant enzyme, as judged by SDS–PAGE and zymography, was greater than 95%, with one distinct band per enzyme preparation (data not shown). No discernible difference was observed in secondary structure between the wild type and the 12 mutant forms of TFsβ-glucanase using fluorescent spectrometry according to the method published previously (Wen *et al.*, 2005). The kinetic properties of the wild type and mutant forms of TFsβ-glucanase were then characterized. The optimal temperature of the mutant and wild-type TFsβ-glucanases was between 313 and 323 K, with an optimal pH of 6 or 8.

The kinetic properties of the wild-type and mutant forms of TFsβ-glucanase were analyzed by determining the rate of reducing-sugar production from the hydrolysis of lichenan. Among the 12 mutants, the most significant change in catalytic activity was seen on mutation of residue Gln70, with a 2.7-fold to 36-fold smaller turnover rate (k_{cat}) and a sixfold to 18.6-fold higher K_m compared with wild-type TFsβ-glucanase. Replacing Gln70 with nonpolar amino-acid residues such as alanine and isoleucine led to the most significant degradation of catalytic function. The mutations Q70A and Q70I had 299-fold and 499-fold lower k_{cat}/K_m ratios than the wild-type enzyme, respectively (Table 3). Substitution of Gln70 with Asp, Asn and Glu decreased the k_{cat}/K_m value by 60-fold to 106-fold. Interestingly, Q70R exhibited a much smaller loss in catalytic efficiency, with a 35-fold decrease. N72A and N72Q had 11-fold and 17-fold lower k_{cat}/K_m ratios than the wild-type enzyme, respectively. Mutation of Gln81 to Ile or Asn only had a moderate effect on the k_{cat} or K_m values. E85I and E85D had a fivefold lower k_{cat}/K_m than the wild type. Taken together, these results show that the amino-acid residues proposed to bind to substrate subsites +1 and +2 of carbohydrate β-D-glucan or lichenan indeed play important roles in the catalysis of TFsβ-glucanase.

Table 3
Kinetic properties of wild-type and mutant TFsβ-glucanase.

Enzyme	Specific activity† (units mg^{-1})	K_m‡ (mg ml^{-1})	k_{cat}‡ (s^{-1})	k_{cat}/K_m (ml s^{-1} mg^{-1})	Interacting carbohydrate
TFsβ-glucanase	8478	2.86	3920	1370.6 (100%)	
Q70A	527	53.2	244	4.59 (0.34%)	Glucose +1
Q70I	236	39.7	109	2.75 (0.20%)	Glucose +1
Q70D	1381	29.0	639	22.0 (1.60%)	Glucose +1
Q70N	802	17.1	371	21.7 (1.58%)	Glucose +1
Q70E	1385	49.6	641	12.9 (0.94%)	Glucose +1
Q70R	3104	36.5	1435	39.3 (2.87%)	Glucose +1
N72A	1774	6.78	820	121 (8.83%)	Glucose +1
N72Q	1089	6.27	504	80.4 (5.87%)	Glucose +1
Q81I	7873	5.14	3641	708 (51.7%)	Glucose +2 *via* water
Q81N	5758	4.95	2663	538 (39.3%)	Glucose +2 *via* water
E85I	1699	2.68	785	293 (21.4%)	Glucose +1, +2
E85D	3076	5.04	1422	282 (20.6%)	Glucose +1, +2

† Reactions were performed with lichenan as the substrate in 50 m*M* sodium citrate buffer pH 6.0, 50 m*M* sodium phosphate buffer pH 7.0 or 50 m*M* Tris–HCl buffer pH 8.0 and at optimal temperatures of 313–323 K for the individual enzymes as characterized in this study. ‡ The standard errors in all the experimental data were less than 5%.

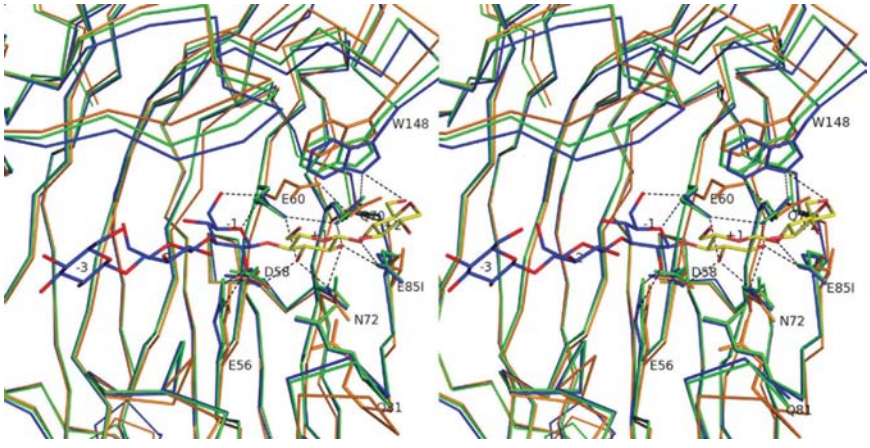

Figure 1
Stereoview of the active site and mutation site of the E85I mutant (orange), TFsβ-glucanase (green) and TFsβ-glucanase–CLTR (blue; CLTR is shown in blue/red) with a model of substrate carbohydrate subunits +1 to +2 (yellow/red). A 12-hydrogen-bond (<3.5 Å) network between carbohydrate subunits +1 to +2 and TFsβ-glucanase (blue) residues Glu56, Asp58, Glu60, Gln70, Asn72, Glu85 and Trp148 is shown by the dotted lines.

3.2. The E85I mutant structure

X-ray diffraction structural analysis was used to obtain new insights into the amino-acid residues that interact with substrate subsites +1 and +2 in all the mutants. Attempts were made to obtain crystals of all the mutants; however, only the E85I mutant crystals were suitable for data collection. In this study, the overall structure of the E85I mutant, which contained residues 3–243,

one calcium ion, one caesium ion and 199 water molecules, was found to be similar to that of the wild type. The structure mainly consists of two antiparallel eight-stranded β-sheets arranged in a jelly-roll β-sandwich with both β-sheets twisted, giving a convex and a concave side to the molecule. The superimposition of C^{α} atoms of three structures, free TFsβ-glucanase (PDB code 1mve), the TFsβ-glucanase–CLTR (product) complex (PDB code 1zm1) and the E85I mutant (PDB code 2r49), are shown in Fig. 2(*a*). In the E85I mutant structure, the four loops *A*–*D* which gate the active site of the enzyme had shifted away from the concave side (Fig. 1), with average r.m.s.d.s of 1.05 and 1.35 Å, respectively, compared with free TFsβ-glucanase (1mve) and the TFsβ-glucanase–CLTR complex (1zm1). Loops *A* (residues 46–53) and *B* (residues 75–83), which are located at the bottom of the active site of the enzyme, had moved ~1.0 Å away from the active site, while the other two loops (loop *C*, residues 142–151, and loop *D*, residues 203–211), which are located above the active site of the E85I mutant enzyme, had moved 1.5–2 Å away from the active site (Fig. 2*b*).

3.3. Crystal packing and conformation changes

The E85I mutant (PDB code 2r49) crystallized in space group $P3_121$ (with one molecule in the asymmetric unit), which is not readily compatible with the free enzyme (PDB code 1mve; space group $P2_12_12_1$) and the complex (PDB code 1zm1; space group $P2_1$). Based on the E85I mutant crystal-

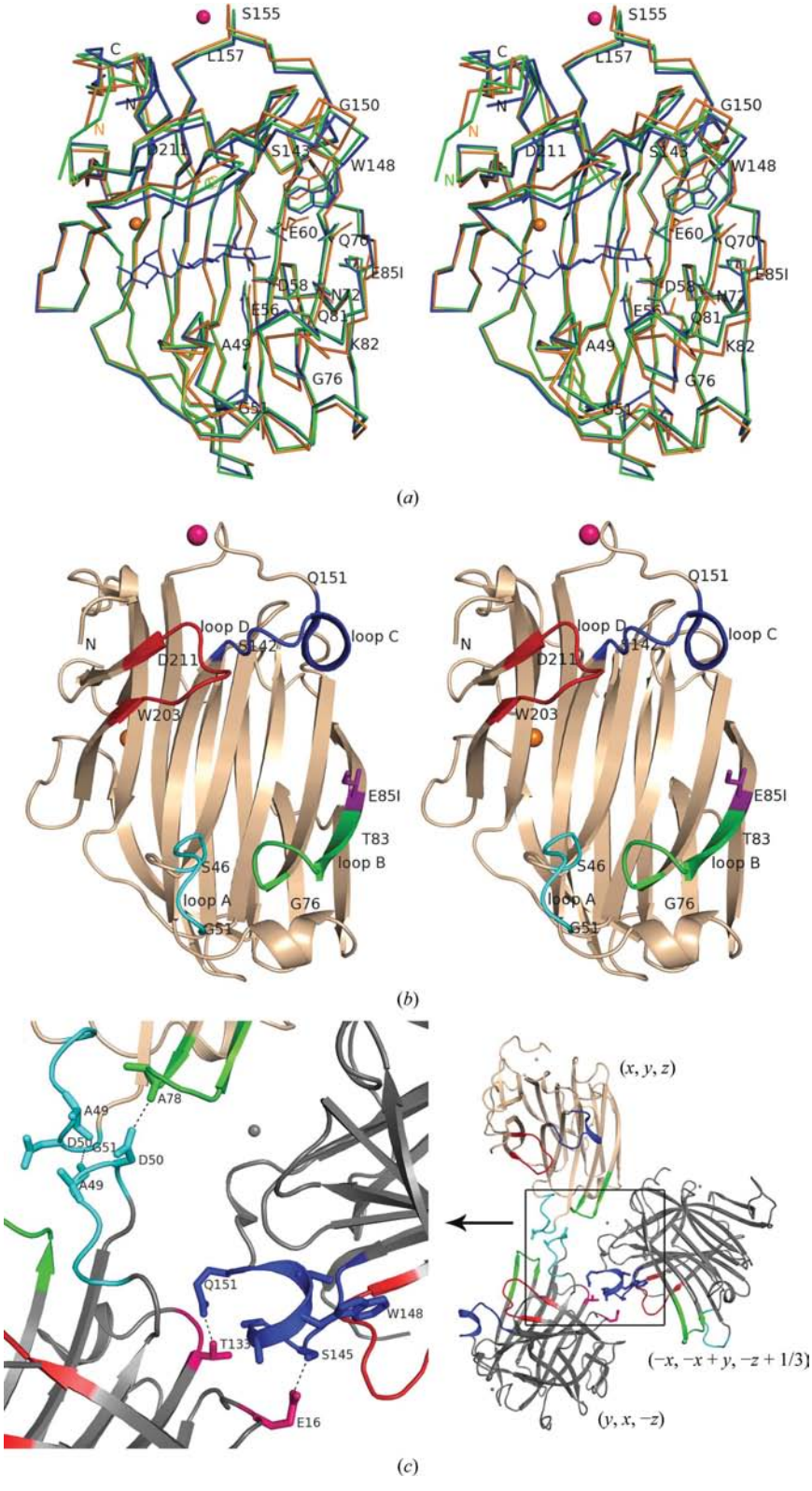

Figure 2
(*a*) Superimposition of the C^{α} atoms of the E85I mutant (orange), TFsβ-glucanase (green) and TFsβ-glucanase–CLTR (blue). The structure is orientated so that the reducing end of the sugar (CLTR) is at the top right of the protein molecule, with two eight-β-stranded antiparallel β-sheets. The mean r.m.s.d.s between the E85I mutant and the free enzyme and the enzyme–product complex are 0.7 and 0.9 Å, respectively, for 230 corresponding C^{α} atoms. Calcium and caesium ions are shown as orange and pink balls, respectively. (*b*) Ribbon drawing of the overall crystal structure of the E85I mutant structure. Loop *A* (residues 49–51, cyan) and loop *B* (residues 72–82, green) located at the bottom of the protein molecule and loop *C* (residues 142–151, blue) and loop *D* (residues 203–211, red) located above the protein molecule are indicated. The E85I mutation site is shown in purple and the calcium ion is shown as a gold ball. (*c*) Left, the crystal-packing interfaces of the E85I mutant molecule and its two symmetry molecules. The residues Gly51 of loop *A* and Ala78 of loop *B* of the E85I mutant molecule (x, y, z) are individually associated with residues Ala49 and Asp50 of loop *A* of the symmetry molecule (y, x, $-z$). The hydrogen-bonding interactions between loop *D* residues Ser145 and Gln151 in the symmetry molecule ($-x$, $-x + y$, $-z + 1/3$) and residues Glu16 and Thr133 of the symmetry molecule (y, x, $-z$) are shown. Right, the monomer in the asymmetric unit is shown in wheat, with two symmetry molecules shown in grey. The loop colours are the same as in Fig. 1(*b*). All figures were produced using *PyMOL* (http://www.pymol.org).

packing symmetry, the loop *A* residue Gly51 and loop *B* residue Ala78 in the monomer (*x*, *y*, *z*) were individually associated with the loop *A* residues Ala49 and Asp50 of the first symmetry molecule (*y*, *x*, $-z$). In addition, loop *C* residues Ser145 and Gln151 of the second symmetry molecule ($-x$, $-x + y$, $-z + 1/3$) make hydrogen-bond interactions with Glu16 and Thr133 of the first symmetry molecule (Fig. 2*c*). However, none of the crystal-packing interfaces mentioned above were found in the free enzyme (space group $P2_12_12_1$) or the complex (space group $P2_1$). We therefore propose that the movement of the four loops was more likely to be a consequence of symmetry packing during crystallization and was not related to caesium-ion binding (discussed below). Although the crystallization led to loop movement, the core structure of the E85I mutant was maintained, demonstrating that the four loops of TFsβ-glucanase are variable.

3.4. The Ca^{2+}- and Cs^{+}-binding sites

One calcium binding site, similar to that in the wild type, is located on the edge of the convex side of the structure and is coordinated by six atoms arranged in an octahedral geometry, namely three backbone carbonyl O atoms (Asn164, Asn189 and Gly222), one of the carboxylate O atoms of Asn164 and two water molecules (Fig. 3*a*). The Ca^{2+} ion-binding sites of Bs glucanase, Pm glucanase and TFsβ-glucanase are thought to stabilize their three-dimensional structures (Hahn *et al.*, 1995; Keitel *et al.*, 1994; Tsai *et al.*, 2003). Although the E85I mutant was crystallized in the absence of Ca^{2+} ions, the Ca^{2+} ion-binding site found in the wild type was maintained. Analysis of the Ca^{2+}-ion concentration in the mutant proteins by polarized Zeeman atomic absorption spectrophotometry showed that the molecular ratio of Ca^{2+} ion to protein in all the purified protein mutants was approximately 2:1. Similarly, one Ca^{2+} ion that was not supplied by the crystallization conditions was found in both the GHF16 β-agarase A and B enzymes (Allouch *et al.*, 2003, 2004). These calcium ions are bound by the protein from the original culture medium, as is the case with the glucanases here.

In addition, a Cs^{+} ion was found near residues Ser155 and Leu157 of the E85I mutant. This was coordinated to five moieties: the carboxyl O atoms of Ser155 and Leu157 and three water molecules (Fig. 3*b*), arranged in a trigonal bipyramidal geometry. The occupancy and *B* factor of the Cs^{+} ion were calculated to be 0.30 and 31.0 Å^2, respectively, using the program *CNS* (Brünger *et al.*, 1998). The low occupancy of the Cs^{+} ion may be because the Cs^{+} ion binding site is located on the surface loop of the protein and coordinates to three water molecules. A similar caesium binding site has been reported in ribonuclease A (Schultz *et al.*, 2005), coordinated to five O atoms, including two tyrosine side-chain and three backbone carbonyl O atoms. Although the ribonuclease A crystal was grown in a high concentration of CsCl (3 *M*), the occupancy of the Cs^{+} ions was 0.46.

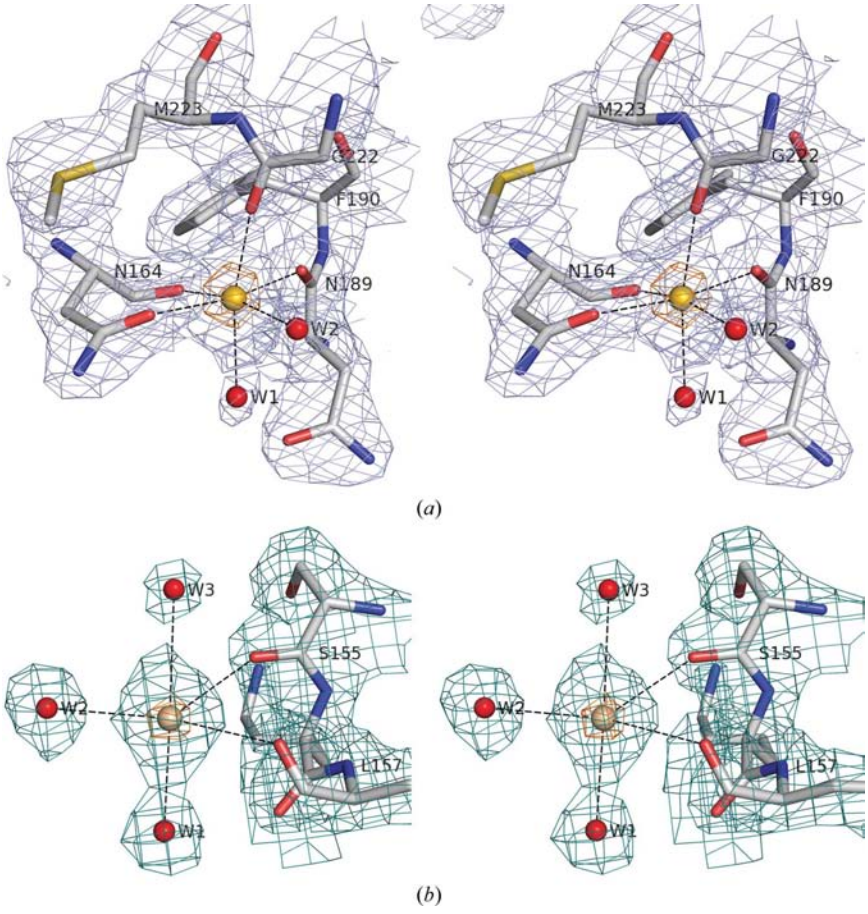

Figure 3
Electron-density map (blue) contoured at 1σ around various Ca^{2+} and Cs^{+} ion binding sites. (*a*) The octahedral geometry calcium binding site in the E85I mutant. The $2F_o - F_c$ Fourier map (orange) is shown at 4σ for the Ca^{2+} ion. (*b*) The caesium ion is coordinated by five atoms: the carboxyl O atoms of Ser155 and Leu157 and three water molecules. The electron-density map (orange) is shown at 6σ for the Cs^{+} ion.

3.5. The active-site residues and the mutation site

Analysis of the crystal structure of TFsβ-glucanase in complex with CLTR showed that residues Glu56 and Glu60 play important roles as a nucleophile and a general acid/base, respectively, in hydrolysis of the β-1,4-glycosidic linkage (Tsai *et al.*, 2005). In order to understand the structural rationale for the recognition of substrate, we mutated several residues, Gln70, Asn72, Gln81 and Glu85, located at the active site and close to the key residues Glu56 and Glu60. The only mutant that we were able to successfully crystallize was the E85I substitution. In OMIT electron-density maps of the site 85 mutation, the isoleucine residue and other

residues in the vicinity are well defined (Fig. 4). However, many other residues, such as Glu60 and Trp148, in the vicinity of the mutation site have moved away from the active site, perhaps owing to crystal-packing constraints. In contrast to the structures of TFsβ-glucanase (Tsai *et al.*, 2003) and TFsβ-glucanase–CLTR (Tsai *et al.*, 2005), the structure of the E85I mutant showed Glu60 C^{γ} to be rotated about 100° away from the active site, but the $C^{\alpha}-C^{\beta}$ bond of Glu60 maintained the same orientation. Residue Trp148 located on loop *C* shifted significantly away from the active site by about 2 Å (see Fig. 1), resulting in configuration changes of the so-called catalytic proton-donor residue Glu60. However, the shift of Glu60 is a consequence of the movement of loop *C*, based on symmetry-molecule interactions. The interactions between symmetry structures may influence the stability of the loops in the E85I mutant. However, the movement of the loops may not directly affect the enzymatic kinetic function since the core structure and the residues in the active site maintain their proper positions. Although Glu60 was shifted away from the active site in the E85I mutant structure when substrate was bound into the active site, we propose that the Glu60 could rotate back to the wild-type position and exclude water molecule W1 from the active site (Fig. 4). This may explain why the E85I mutant showed a fivefold difference in k_{cat}/K_m with a similar affinity K_m as the wild type (Table 3). Our previous studies showed that Glu85 $O^{\varepsilon1}$ formed two hydrogen bonds to the O3 atom of glucose +1 and the O4 atom of glucose +2 of the modelled substrate carbohydrate in TFsβ-glucanase–CLTR (Tsai *et al.*, 2005; Fig. 1). Abolishing these two hydrogen bonds in the E85I mutant had a minor influence on enzyme hydrolysis, indicating that Glu85 is not directly involved in enzyme function.

In addition, minor structural differences occurred at residues Gln70 and Asn72, which are associated with glucose +1 of the modelled substrate carbohydrate (Fig. 1). This movement may affect the enzymatic properties because the core structure and the residues in the active site remained in their proper positions. In the wild-type structure, Gln70 $N^{\varepsilon2}$ and Gln70 $O^{\varepsilon1}$ made two hydrogen bonds to the catalytic residue Glu60 $O^{\varepsilon2}$ (3.5 Å) and Trp148 $N^{\varepsilon1}$ (3.1 Å), respectively. This hydrogen-bond network holds residues Glu60, Gln70 and Trp148 in a strained configuration. In the E85I mutant, loop *C* (residues 141–150) shifted away from the active site by about 1.8 Å, which abolished the hydrogen bond between Trp148 $N^{\varepsilon1}$ and Gln70 $O^{\varepsilon1}$. However, the hydrogen bond between Gln70 $N^{\varepsilon2}$ and Glu60 $O^{\varepsilon2}$ became shorter (decreasing from 3.5 to 2.7 Å). The movement of Glu60 in the E85I mutant created space for a water molecule (W1 in Fig. 4). From our kinetic study of the active-site residues (Table 3), Gln70 and Asn72 play the most important roles in kinetic function: Gln70 not only binds to the catalytic residue Glu60 but also interacts with substrate unit +1 (Fig. 1), and Gln70 and Asn72 are located in the core of the active site.

In summary, differences in the residues in the active-site region of glycosyl hydrolases create binding-site topographies that require different substrate conformations. The active-site residues in TFsβ-glucanase form a specific topology which accommodates mixed β-1,4- and β-1,3-glycosidic linkages in lichenan or β-D-glucan subunits −3 to +2 *via* many hydrogen bonds and stacking interactions. Mutation of the active-site residues may decrease the interaction affinity between the enzyme and the substrate and reduce the catalytic function of the enzyme. Residue Gln70 formed two hydrogen bonds: one to substrate subunit +1 and another to the catalytic residue Glu60, which may hold Glu60 in the proper orientation. This may explain why the mutation of Gln70 resulted in such low enzymatic function: Gln70 not only interacts with the substrate but also plays an important structural role in constraining the proposed general acid/base residue Glu60 in the correct position for carbohydrate hydrolysis. We propose that the variable positions of the loops that lie on either side of the active site in the crystal forms may also be variable in the solvated form of the protein. The symmetrical interactions shown in this study imply that the loops of TFsβ-glucanase are variable without changing the main core structure in which the active site is situated.

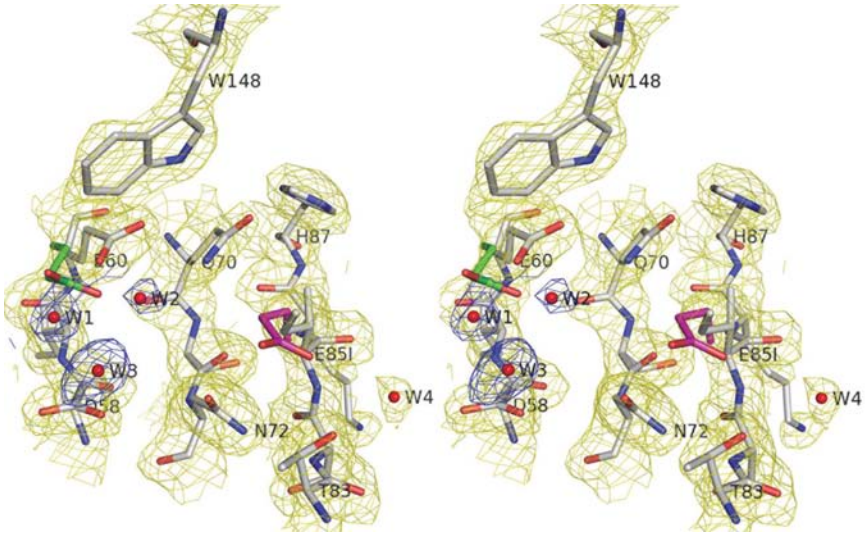

Figure 4
Stereoview of the OMIT $2F_o - F_c$ electron density at 1σ at the mutation-site residue 85 (Glu85 shown in purple) of the the E85I mutant at 2.2 Å resolution. The protein is shown in brown and three water molecules (red balls highlighted with a blue map) surround the catalytic residue Glu60. Glu60 (green/red) was present in the wild type, shifted away from the active site, and a water molecule W1 occupied the position in the E85I mutant. The C^{γ}, C^{δ}, $O^{\varepsilon1}$ and $O^{\varepsilon2}$ atoms of Glu60 were rotated away from the active site of the protein. Residue 85 was omitted from the map calculation.

This work was supported by research grants from National Taipei University of Technology and the National Science Council (NSC95-2311-B-027-001). We would like to thank Dr Carmay Lim for useful discussions.

References

Allouch, J., Helbert, W., Henrissat, B. & Czjzek, M. (2004). *Structure*, **12**, 623–632.

Allouch, J., Jam, M., Helbert, W., Barbeyron, T., Kloareg, B., Henrissat, B. & Czjzek, M. (2003). *J. Biol. Chem.* **278**, 47171–47180.

Anderson, M. A. & Stone, B. A. (1975). *FEBS Lett.* **52**, 202–207.

Bedford, M. R., Patience, J. F., Classen, H. L. & Inborr, J. (1992). *Can. J. Anim. Sci.* **72**, 97–105.

Brünger, A. T., Adams, P. D., Clore, G. M., DeLano, W. L., Gros, P., Grosse-Kunstleve, R. W., Jiang, J.-S., Kuszewski, J., Nilges, M., Pannu, N. S., Read, R. J., Rice, L. M., Simonson, T. & Warren, G. L. (1998). *Acta Cryst.* D**54**, 905–921.

Cerny, J. & Hobza, P. (2007). *Phys. Chem. Chem. Phys.* **9**, 5291–5303.

Chen, H., Li, X. L. & Ljungdahl, L. G. (1997). *J. Bacteriol.* **179**, 6028–6034.

Chen, J.-L., Tsai, L.-C., Wen, T.-N., Tang, J.-B., Yuan, H. S. & Shyur, L.-F. (2001). *J. Biol. Chem.* **276**, 17895–17901.

Cheng, H.-L., Tsai, L.-C., Lin, S.-S., Yuan, H. S., Lee, S.-H. & Shyur, L.-F. (2002). *Biochemistry*, **41**, 8759–8766.

Davies, G. & Henrissat, B. (1995). *Structure*, **3**, 853–859.

Dennis, R. J., Taylor, E. J., Macauley, M. S., Stubbs, K. A., Turkenburg, J. P., Hart, S. J., Black, G. N., Vocadlo, D. J. & Davies, G. J. (2006). *Nature Struct. Mol. Biol.* **13**, 365–371.

Gaiser, O. J., Piotukh, K., Ponnuswamy, M. N., Planas, A., Borriss, R. & Heinemann, U. (2006). *J. Mol. Biol.* **357**, 1211–1225.

Hahn, M., Pons, J., Planas, A., Querol, E. & Heinemann, U. (1995). *FEBS Lett.* **374**, 221–224.

Henrissat, B. (1991). *Biochem. J.* **280**, 309–316.

Henrissat, B. & Bairoch, A. (1993). *Biochem. J.* **293**, 781–788.

Keitel, T., Meldgaard, M. & Heinemann, U. (1994). *Eur. J. Biochem.* **222**, 203–214.

Keitel, T., Simon, O., Borriss, R. & Heinemann, U. (1993). *Proc. Natl Acad. Sci. USA*, **90**, 5287–5291.

Li, G., Zhao, G., Schindelin, H. & Lennarz, W. J. (2008). *Biochem. Biophys. Res. Commun.* **375**, 247–251.

Miller, G. L. (1959). *Anal. Chem.* **31**, 426–428.

Müller, J. J., Thomsen, K. K. & Heinemann, U. (1998). *J. Biol. Chem.* **273**, 3438–3446.

Otwinowski, Z. & Minor, W. (1997). *Methods Enzymol.* **276**, 307–326.

Rajan, S. S., Yang, X., Collart, F., Yip, V. L. Y., Withers, S. G., Varrot, A., Thompson, J., Davies, G. J. & Anderson, W. F. (2004). *Structure*, **12**, 1619–1629.

Rao, F. V., Dorfmueller, C. H., Villa, F., Allwood, M., Eggleston, I. M. & van Aalten, D. M. F. (2006). *EMBO J.* **25**, 1569–1578.

Roussel, A. & Cambillau, C. (1992). *The TURBO-FRODO Graphics Package. Silicon Graphics Geometry Partners Directory*, Vol. 81. Mountain View, USA: Silicon Graphics.

Sacquin-Mora, S., Carbone, A. & Lavery, R. (2008). *J. Mol. Biol.* **382**, 1276–1289.

Schultz, D. A., Friedman, A. M., White, M. A. & Fox, R. O. (2005). *Protein Sci.* **14**, 2862–2870.

Selinger, L. B., Forsberg, C. W. & Cheng, K. J. (1996). *Anaerobe*, **2**, 263–284.

Tsai, L.-C., Chen, Y.-N. & Shyur, L.-F. (2008). *J. Comput. Aided Mol. Des.* doi:10.1007/s10822-008-9228-1.

Tsai, L.-C., Shyur, L.-F., Cheng, Y.-S. & Lee, S.-H. (2005). *J. Mol. Biol.* **354**, 642–651.

Tsai, L.-C., Shyur, L.-F., Lee, S.-H., Lin, S.-S. & Yuan, H. S. (2003). *J. Mol. Biol.* **330**, 607–620.

Varghese, J. N., Garrett, T. P. J., Colman, P. M., Chen, L., Hoj, P. B. & Fincher, G. B. (1994). *Proc. Natl Acad. Sci. USA*, **91**, 2785–2789.

Wen, T.-N., Chen, J.-L., Lee, S.-H., Yang, N.-S. & Shyur, L.-F. (2005). *Biochemistry*, **44**, 9197–9205.